batteries

MDPI

Article

Optimization of Retired Lithium-Ion Battery Pack Reorganization and Recycling Using 3D Assessment Technology

Wan Chen [1], Jiaoyue Su [1], Lei Shen [2], Xinfa Gu [1], Junjie Xie [1], Na Sun [1], Hui Huang [1] and Jie Ji [1,*]

[1] Electric Engineering Department, Automatic Faculty, Huaiyin Institute of Technology, Huaiyin 223002, China; calvinchen@hyit.edu.cn (W.C.); su1046197736@outlook.com (J.S.); 11150031@hyit.edu.cn (X.G.); 11180011@hyit.edu.cn (J.X.); zero1437@hyit.edu.cn (N.S.); huanghui@hyit.edu.cn (H.H.)

[2] Huaian Hongneng Group Corp, Huaian 223002, China; shenlei@js.sgcc.com.cn

* Correspondence: jijie@hyit.edu.cn

Abstract: This study introduces a sophisticated methodology that integrates 3D assessment technology for the reorganization and recycling of retired lithium-ion battery packs, aiming to mitigate environmental challenges and enhance sustainability in the electric vehicle sector. By deploying a kernel extreme learning machine (KELM), variational mode decomposition (VMD), and an advanced sparrow search algorithm (SSA), the research achieves a marked increase in the precision of battery classification and performance forecasting. Implementing a three-dimensional dynamic evaluation model, the study optimizes battery pack grouping strategies, culminating in superior secondary utilization rates, extended operational lifespans, and minimized ecological footprints. The research demonstrates that balanced weight distribution strategies, which maximize energy density to 61.37571 Wh/L and cycle counts up to 947 cycles, are pivotal for the efficient reorganization of battery packs, substantiating the economic feasibility and environmental sustainability of recycling initiatives. Future endeavors will extend this research to investigate the influence of diverse battery materials and morphologies on reorganization efficacy, with the aim of broadening the application horizons to include real-world scenarios, thereby refining battery performance and lifespan predictions and propelling forward the frontiers of recycling technology and policy development.

Keywords: reuse of retired battery packs; state of health (SOH); battery recycling and reuse; three-dimensional (3D) assessment model; VMD-SSA-KELM

Citation: Chen, W.; Su, J.; Shen, L.; Gu, X.; Xie, J.; Sun, N.; Huang, H.; Ji, J. Optimization of Retired Lithium-Ion Battery Pack Reorganization and Recycling Using 3D Assessment Technology. *Batteries* **2024**, *10*, 376. https://doi.org/ 10.3390/batteries10110376

Academic Editors: Rodolfo Dufo-López and George Zheng Chen

Received: 7 August 2024
Revised: 10 September 2024
Accepted: 15 October 2024
Published: 24 October 2024

1. Introduction

With the increasing global awareness of sustainable energy and environmental protection [1], battery technology, especially lithium-ion battery technology, has seen rapid growth in applications in electric vehicles (EVs) and energy storage systems (ESSs) [2]. However, in the coming years, there will be a large number of retired electric vehicles, and the limited lifespan of batteries poses a potential threat to the environment [3]. China, as one of the main markets for electric vehicles, plays a crucial role in the research and policymaking concerning the recycling of Lithium-ion batteries. This urgency has made battery recycling and reuse an imperative research topic [4]. This study aims to explore a systematic methodology for the reorganization of retired battery packs to increase the secondary utilization rate of batteries, reduce environmental impact, and provide economically feasible solutions for the battery recycling industry [5].

Internationally, many developed countries have established comprehensive battery recycling systems [6]. In Europe, legislation requires battery manufacturers to be responsible for recycling and disposing of batteries, while also encouraging the adoption of advanced technologies to improve material recovery rates [7]. Similar recycling systems exist in North America, where incentives and the establishment of recycling facilities have promoted battery recycling [8]. Japan, through technological innovation, has developed a combined wet and pyro-metallurgical recycling process, effectively increasing the recovery efficiency

of rare metals in lithium-ion batteries [9], and demonstrating international attention to battery recycling. Nationally, as the world's largest producer and consumer of lithium-ion batteries, China has achieved significant progress in researching and developing battery recycling and reuse technologies. The Chinese government has implemented a series of policies to encourage and support the development of the battery recycling industry, such as the "Management Measures for the Recycling and Utilization of Lithium-ion battery of New Energy Vehicles" [10]. Beijing's policy recommendations and research on battery recycling mechanisms provide valuable experience and insights for other regions. Domestic research institutions and enterprises are actively exploring new methods for battery recycling, including physical, chemical, and biological methods, aiming to improve recycling efficiency and reduce costs [11]. In the field of battery recycling and reuse, recent research has continuously advanced technology and policy. Particularly in the realm of second-life applications for retired lithium-ion batteries (LIBs) used in electric vehicles (EVs), innovators have proposed various cutting-edge methods. For instance, Liu et al. [12] introduced a strategy based on real-time reconfiguration aimed at maximizing the flexibility and capacity utilization of second-life batteries. By dynamically adjusting the battery management system (BMS), this strategy optimizes the configuration of battery packs based on their actual conditions, thereby extending their service life and enhancing energy efficiency. Furthermore, examining the perspective of extended producer responsibility (EPR), researchers in Taiwan have delved into the recycling and reuse of LIBs [13]. They analyzed how EPR policies influence the battery recycling industry and proposed a suite of incentives to encourage participation from battery manufacturers and consumers alike. These studies not only offer fresh insights into LIB recycling but also provide valuable guidance for policymakers. Regarding the assessment of battery state of health (SOH), Wang et al. [14] developed a machine-learning-based SOH prognosis model capable of accurately predicting the remaining useful life (RUL) of batteries. By integrating real-time operational data with historical maintenance records, this model significantly improves the accuracy of SOH forecasting. Such research provides a robust tool for battery health management and maintenance.

Essential to modern society, batteries as energy storage devices experience performance degradation over time and through cycles, ultimately necessitating their retirement [15]. Improper handling of retired batteries not only wastes valuable resources but also poses a serious threat to the ecological environment [16]. Therefore, effective reorganization and reuse of these retired batteries are of significant social, economic, and environmental value in alleviating resource scarcity and reducing environmental pollution [16]. Currently, despite advancements in battery recycling and reuse, there are still challenges to overcome [17]. Emerging technologies such as physical, chemical, and biological methods, as mentioned by Qiao et al., provide new perspectives and technical support for battery recycling, with the potential to increase efficiency and lower costs [18]. Hu's [19] research emphasizes the application of big data in battery recycling, suggesting that establishing an information-sharing platform and optimizing intelligent transportation can enhance the efficiency of battery recycling and reuse. The literature primarily explores large-scale retired lithium-ion battery cascaded utilization energy storage systems, proposing the dynamic reconfigurable battery network (DRBN) technology, which effectively enhances the consistency and safety of such systems. Through the analysis of a practical large-scale retired lithium-ion battery cascaded utilization energy storage system, the role of the DRBN energy storage system in module balancing was verified, offering a new solution for the cascaded utilization of retired lithium-ion batteries [20]. However, there is a lack of research on the variation of state of health (SOH) with usage and time. Moreover, considerations for factors such as different battery brands, shapes, charge/discharge power, and capacity are lacking [19].

These studies demonstrate that assessing the state of health (SOH) of batteries and developing strategies for reorganization and reuse at the battery pack level significantly impact the regrouping of battery packs. Accurate prediction of the SOH of batteries plays a crucial role in the recycling and reorganization of retired batteries. The SOH of a battery is a key indicator for evaluating battery performance and determining whether it is suitable for continued use or in need of recycling. Zou Feng studied an online estimation method for battery SOH based on the dual Kalman filter algorithm and experimentally validated the effectiveness of the algorithm [21]. Wang Ping proposed a joint estimation method for SOH and remaining useful life (RUL) based on Gaussian process regression (GPR) [22]. Wu Zhanyu discussed defining SOH using characterization parameters of battery aging such as capacity, internal resistance, and power [23]. However, these studies show poor stability and reliability in SOH prediction, with high computational costs.

The choice of prediction method significantly influences the accuracy of SOH predictions for batteries [24]. The ISSA-ELM algorithm, by combining a simplified swarm search algorithm with an extreme learning machine (ELM), increases computational [25] complexity while reducing computation speed, but provides more accurate predictions when dealing with complex data patterns and adapting to battery state changes. In contrast, the traditional ELM algorithm has a simple structure, fast training speed, and is suitable for real-time applications requiring quick responses. The kernel extreme learning machine (KELM) is suitable for analyzing time-series data with volatility, nonlinearity, and push-pull trends, and can quickly handle nonlinear problems. Combining it with the SSA algorithm further increases prediction accuracy [26]. For retired batteries, their SOH undergoes certain decay, presenting nonlinear problems. Moreover, there are multiple brands of retired battery packs with complex data, adding difficulty to accurate prediction. Therefore, choosing the most suitable algorithm requires a comprehensive consideration of application scenarios, data characteristics, and performance requirements to ensure efficient and accurate SOH estimation in battery management systems. Variable mode decomposition (VMD) is an adaptive signal processing technique that decomposes complex signals into a series of intrinsic modal functions (IMFs) with finite bandwidth, making it well-suited for predicting the performance of retired battery packs, which often exhibit high internal resistance and interference [27].

Furthermore, rational grouping decisions also significantly influence battery recycling and reuse [28]. By considering key features such as brand, shape, charge/discharge power, and capacity, effective classification of batteries based on similar performance parameters can enhance the consistency and reliability of battery pack groups [29]. This approach not only improves battery pack design but also optimizes space utilization and thermal management efficiency and increases the cycle life of battery pack groups. Conversely, mixing batteries with significant feature differences may lead to decreased efficiency in battery packs due to inconsistent charge/discharge characteristics, difficult thermal management, noticeable lifespan variations, large differences in maximum capacity within the pack group, and challenges in balancing individual battery handling [30]. This can reduce the lifespan of batteries with better state of health, increase costs, and hinder the overall performance and economic benefits of the reorganized battery packs. Therefore, rational grouping decisions play a significant role in ensuring performance, extending the lifespan, increasing the cycle count, improving versatility, and enhancing the economic benefits of reorganized battery packs [31].

Currently, there are numerous assessments targeting individual battery packs on the market. However, with the rapid growth of electric vehicles leading to a surge in retired lithium-ion batteries, the importance of accurately evaluating the performance of reorganized battery packs is becoming increasingly prominent, both for environmental demands and economic value considerations [32]. The evaluation of a battery pack group involves not only the health status, capacity, and lifespan of the batteries but also the establishment of the battery management system (BMS) [33], which is crucial for ensuring the safe operation of the reorganized battery packs [34]. Moreover, the reorganization and

reuse at the battery pack group level require a comprehensive consideration of various factors such as different brands, shapes, charge and discharge power, and capacities to achieve efficient reassembly of the battery packs [35]. The three-dimensional transient numerical model assessment method mentioned by Sun Zeyu provides a new methodological approach for the performance evaluation of battery pack groups, which helps to enhance the efficiency and service life of the reorganized battery packs [36]. The recycling process analysis and cost estimation by Kou Farong further emphasize the key role of battery pack group evaluation in battery recycling decision-making [37]. Therefore, the evaluation of battery pack groups plays a vital role in promoting the sustainable development of the battery recycling industry.

The primary objective of this study is to enhance the secondary utilization rate of retired lithium-ion battery packs by developing a systematic methodology for their reorganization and recycling. This involves integrating advanced analytical techniques such as KELM [38], VMD, and improved sparrow search algorithms (SSA) to accurately assess the state of health (SOH) and optimize battery pack regrouping strategies. Our goal is to demonstrate how these methods can significantly improve the operational lifespan and energy density of repurposed battery packs, thereby contributing to more sustainable and economically viable battery recycling solutions. Through the establishment of a 3D evaluation model [39], a comprehensive performance assessment of the restructured battery packs is conducted to find a reasonable grouping strategy to improve the secondary utilization of the batteries, enhance the performance and service life of the restructured battery packs, reduce the environmental impact, and provide an economically feasible solution for the battery recycling industry. Through these studies, this paper expects to provide new perspectives and technical support for the recycling and reuse of retired batteries, and to promote the sustainable development of the battery industry.

2. Methodology

The reassembly of retired battery packs begins with a meticulous recycling and classification process, as depicted in Figure 1. The initial step in our methodology is the meticulous recycling and classification of retired battery packs, ensuring that each pack is meticulously assessed and categorized based on its unique attributes, such as type, brand, shape, volume, and health status. This systematic approach facilitates the optimization of subsequent reorganization processes, aligning with our comprehensive strategy for enhancing the secondary utilization and lifespan of batteries.

Furthermore, by ensuring a uniform health status among batteries in each pack, we streamline the management of battery packs post-reassembly. Figure 1 illustrates the comprehensive flowchart of our decommissioned battery reorganization method, highlighting the steps from initial assessment to final reassembly. This flowchart not only guides the reassembly process but also serves as a visual representation of our research methodology, ensuring the transparency and reproducibility of our approach.

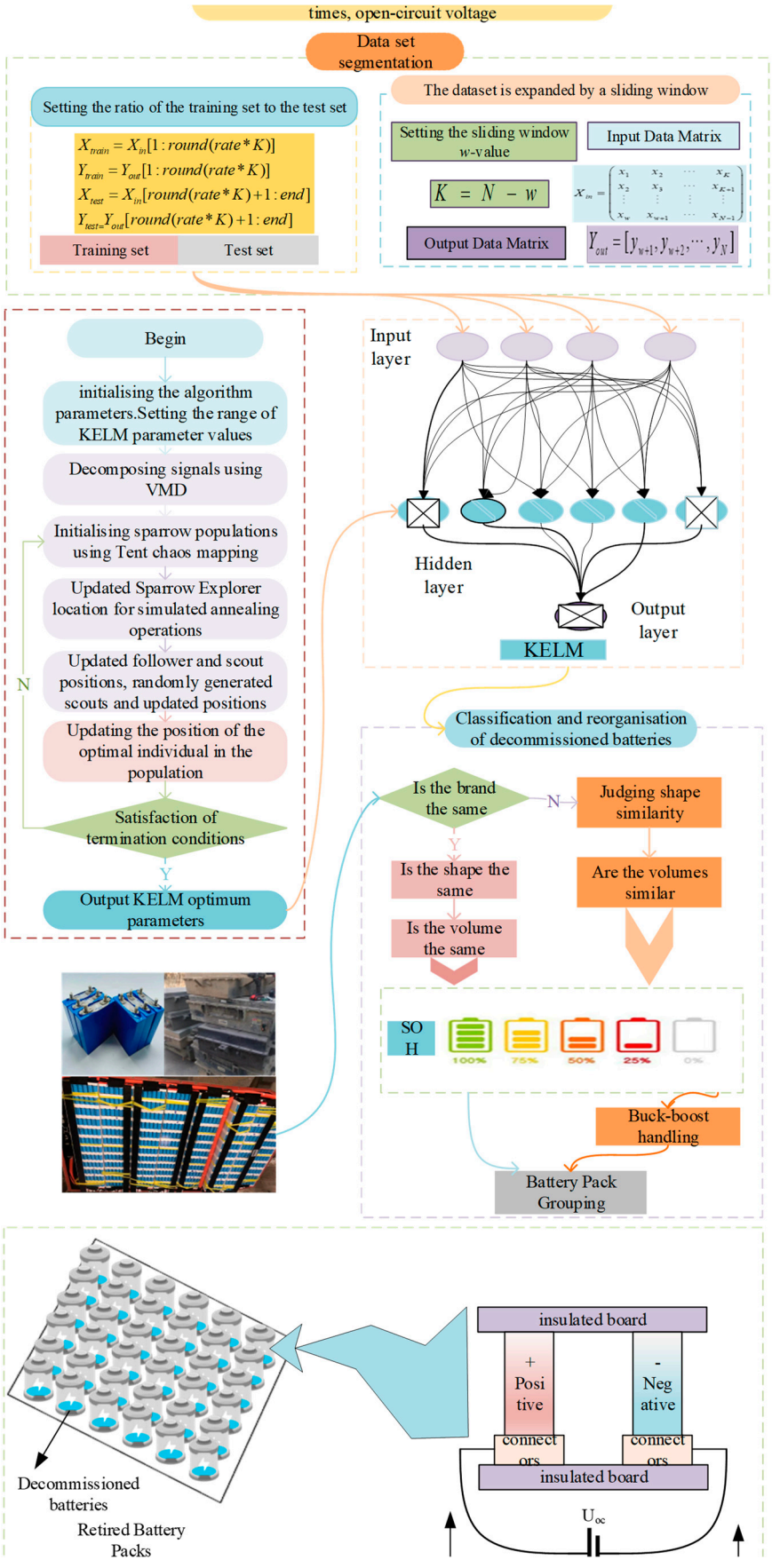

Figure 1. Flowchart of proposed decommissioned battery reorganization method.

2.1. Assessment of Battery State of Health SOH

A novel prediction method based on VMD is used in the health state assessment of decommissioned battery packs. VMD is an adaptive signal processing method that is able to decompose complex signals into a series of intrinsic modal functions (IMFs) with finite bandwidth. This method is widely used in the field of signal processing to extract the intrinsic modes of a signal. The combination of SSA and KELM allows the construction of a powerful predictive model for applications such as predicting battery health status. This approach first decomposes the battery charge/discharge data using VMD, which decomposes the complex nonlinear signal into a number of intrinsic mode functions (IMFs), each representing a periodic component of the data. In this way, noise can be effectively removed and key features of battery performance can be extracted.

2.1.1. KELM Forecast

Lithium batteries play an important role in the field of transportation and energy storage, and accurate assessment of lithium battery health status is of great significance for the application of decommissioned battery pack combinations. KELM makes up for the defects of ELM [40], which requires more implicit layer nodes, by introducing kernel functions in order to improve the prediction accuracy, generalization performance, and stability, and alleviates the computational burden and the problem of increased stochasticity.

The KELM kernel Ω_{ELM} matrix is defined as:

$$\begin{cases} \Omega_{ELM} = HH^T \\ \Omega_{ELM} = h(x_i)h(x_j) = K(x_i, x_j) \end{cases} \tag{1}$$

$$K(x_i, x_j) = \exp(-S\|x_i - x_j\|), S > 0 \tag{2}$$

where $h(x)$ is the output matrix of the implicit layer, $h(x) = H$ is the generalized inverse matrix of matrix H, H^T is the kernel function, $K(x_i, x_j)$ is the generally selected RBF kernel function as the kernel matrix factor, and S is the number of kernel functions. The output variable function is expressed by the following equation:

$$\begin{cases} \beta = H^T(I/C + HH^T)^{-1}Q \\ f(x) = h(x)\beta = \begin{bmatrix} K(x, x_1) \\ \vdots \\ K(x, x_p) \end{bmatrix}^T (I/C + \Omega_{ELM})^{-1}Q \end{cases} \tag{3}$$

where I is the diagonal matrix; C is the regularization coefficient, which is the tolerance of the relative error and affects the KELM performance; β is the output weight; and Q is the desired output.

KELM's pre-set kernel function can avoid the optimization time of the number of neurons in the hidden layer, and the two most critical parameters are the kernel function parameter S and the regularization coefficient C, which determine the data distribution mapped to the new feature space and the tolerance of the relative error, respectively, which improves the decrease in generalization and stability caused by the random assignment of the hidden layer neurons in the hidden layer and reduces the impact of its randomness. In order to make the prediction of KELM more accurate, optimization of the S and C parameters is carried out using the improved sparrow search algorithm, which improves the algorithm's optimization-seeking ability, making it possible to obtain more accurate model parameters in KELM.

2.1.2. SSA Improvements

In this paper, the steps of the algorithm improvement program are as follows:

(1) Tent chaotic mapping can effectively improve the problem of poor uniformity and diversity of randomly generated sparrow populations. The chaotic mapping Tent chaotic mapping mathematical expression is:

$$X_{ij} = a + (b - a)M_K \tag{4}$$

$$M_{K+1} = \begin{cases} 2M_K, 0 \le M_K \le 0.5 \\ 2(1 - M_K), 0.5 < M_K \le 1 \end{cases} \tag{5}$$

where M_K is the value of the mapping function at the kth iteration; X_{ij} is the population of parent sparrows obtained after Tent chaotic mapping; and a and b are the minimum and maximum values, respectively.

(2) The simulated annealing operation is to receive the new state, i.e., the non-optimal solution, with appropriate probability. Using this idea to update the explorer population in sparrows can increase the probability of jumping out of a local optimum and improve the optimality-seeking ability of SSA. During SSA iteration, the value of the fitness function corresponding to the optimal solution increases, and the probability P that this optimal solution is received is:

$$P = \begin{cases} 1 & , f(\lambda) < f(\lambda - 1) \\ \min\left[\exp\left(-\frac{f(\lambda) - f(\lambda-1)}{T_\lambda}\right), 1\right] > \eta & f(\lambda) > f(\lambda - 1) \end{cases} \tag{6}$$

where $f(\lambda)$ is the value of the fitness function at iteration t; exp is a random number between (0, 1); and T_λ is the temperature control coefficient, which is expressed as:

$$T_\lambda = \delta T_{\lambda - 1} \tag{7}$$

where δ is the temperature cooling coefficient, the value of which is generally taken as 0.8 to 0.99.

Lithium battery SOH is very important for retired battery pack restructuring and the more similar the battery capacity and life, the more similar the restructured battery pack. Retired battery pack capacity utilization assessment is a prerequisite for the restructuring of retired batteries and gradient utilization.

2.1.3. VMD

The battery operating data is first pre-processed, including denoising and normalization, to improve the accuracy of the subsequent analysis, and then, the pre-processed signal is decomposed into multiple intrinsic modal functions (IMFs) by using the VMD algorithm, with each IMF representing a specific frequency component of the signal. SSA analysis is performed on each IMF to identify periodic patterns and trends in the signal. From the SSA analysis, features are extracted that reflect key information about the battery health state, these features are input into KELM, the KELM model is trained with a training dataset, the trained KELM model is applied to new battery data and the performance of the model is evaluated using a validation dataset, and the final output is the prediction of the battery health state.

The variational problem solution can be expressed as:

$$J(u) = \frac{1}{2}\int_{-\infty}^{\infty} \|u(\lambda) - s(\lambda)\|^2 d\lambda + \alpha \sum_{k=1}^{K} \int_{-\infty}^{\infty} \left(\omega_k^2(\lambda) - \omega_{k0}^2\right)^2 d\lambda \tag{8}$$

where $u(\lambda)$ is the decomposed IMF, $s(\lambda)$ is the original signal, $\omega_k(\lambda)$ is the frequency of the IMF, ω_{k0} is the center frequency, α is the penalty factor, and K is the number of IMFs.

2.1.4. Three-Dimensional Assessment

This is used to determine the health status of the recycled Li-ion battery cells when the Li-ion battery cell life or maximum charge is between 50% and 60%.

According to [41], the retired battery pack capacity utilization assessment model can be obtained as:

$$\zeta = \frac{E_{S-N}}{E_N} \times 100\% = 0.8347 - 2.6043 \times 10^{-5} \times n \tag{9}$$

where ζ denotes the available capacity rate; E_{S-N} denotes the current available capacity/kWh of the battery pack; E_N denotes the maximum available capacity/kWh of the battery pack; and n denotes the equivalent number of cycles of the battery in one day.

$$E_{S-N} = \sum_{i=1}^{N} \int_{t_0}^{t_0+\Delta t} \left(U_{OCV,i} I - R_i I^2 \right) \mathrm{d}t \tag{10}$$

where U_{OCV} denotes the open-circuit voltage/KV corresponding to a single cell; t denotes the discharge time of the battery pack; and N denotes the number of single cells.

The relationship between the internal resistance of the battery and the SOC is:

$$U_{OCV} = 3.81 - 0.022(-\ln(SOC))^{2.1} + 0.31SOC + 0.07e^{30(SOC-1)} \tag{11}$$

Thus, the current available capacity of the battery pack is:

$$E_{S-N} = \sum_{i=1}^{N} (3.81 - 0.022(-\ln(SOC))^{2.1} + 0.31SOC + 0.07e^{30(SOC-1)})_i Q_i \tag{12}$$

The energy storage battery loss is related to its own charging and discharging depth, charging and discharging multiplicity, and ambient temperature. In [41], the energy storage battery life loss model is introduced in detail, from which it can be seen that the usable capacity of the energy storage battery is mainly determined by the depth of discharge (DOD), so this paper mainly considers the impact of DOD on the usable capacity of the battery. According to the equivalent cycle life method, the maximum number of cycles corresponding to different depths of discharge in the actual operation of the battery is converted into the equivalent number of cycles under the full charging and discharging state (D = 1) and summed to obtain the equivalent number of cycles of the battery in the operation cycle (i.e., one day) n' as:

$$n' = \sum_{g=1}^{n} \frac{4700}{N_{etf}(D) = 6380D^{-0.3614} - 1680} \tag{13}$$

where $N_{etf}(D)$ denotes the maximum number of cycles corresponding to the depth of discharge D of the battery.

It is assumed that the equivalent number of cycles before and after the reorganization of the retired battery is n, n_1', so the service life of the battery is:

$$m = \frac{n_1' - n}{365n'} \tag{14}$$

2.2. Classification and Reorganization of Decommissioned Batteries

The recycled battery packs are categorized by establishing a battery management system (BMS) to ensure that all batteries can be efficiently utilized.

When using the KNN algorithm, the battery packs are classified according to criteria such as battery health status, shape, volume, and brand. Information relating to these criteria is collected and processed as shown in Figure 2.

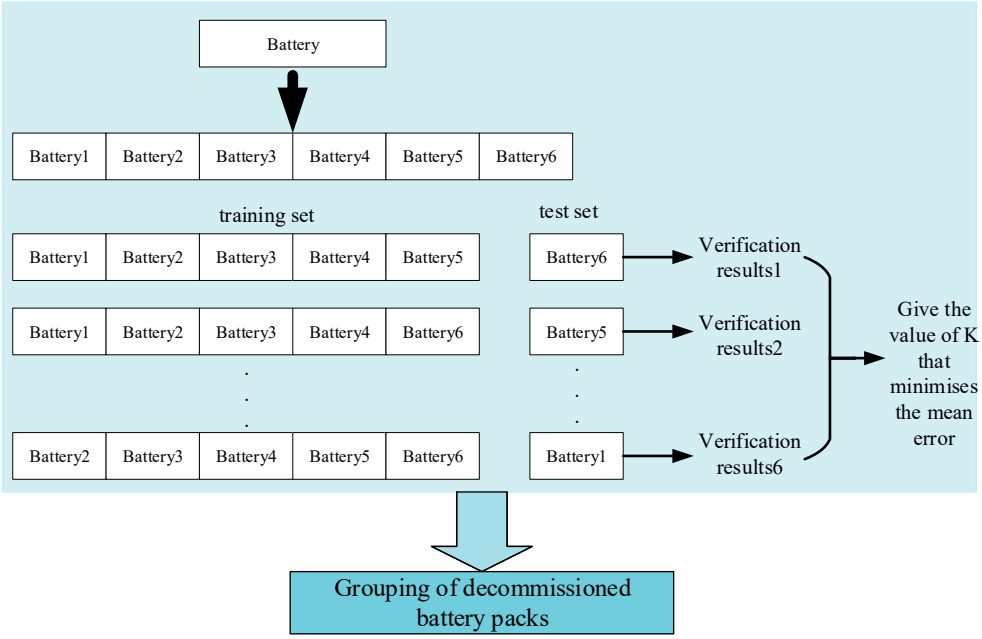

Figure 2. Schematic diagram of grouping strategy for decommissioned battery packs.

2.2.1. Data Processing

Datasets are collected containing features such as battery health status, shape, volume, standard voltage, and brand. The data are standardized or normalized to ensure that individual features (shown in Tables 1 and 2) have the same importance.

Table 1. Battery classification features.

Feature	Description	Type	Instantiation
SOH	state of health	Float	37%
Sf	shape	Float	1 (squareness)
Sb	brand	Float	LFP
Sv	volume	Float	29 × 148 × 98 mm
Sq	quality	Float	900 g
Sc	rated capacity	Float	55 A
Sp	price	Float	100

Table 2. Battery Health Status and Maintenance Prices.

SOH	S_{PW} (Yuan/kWh/Year)
1	7
0.9	18
0.8	34
0.7	101
0.6	313

S_{PW} for battery maintenance costs.

2.2.2. Constructing a KNN Model for Decommissioned Battery Packs

In this step, we specify the K value (number of nearest neighbors) and the distance metric, set the weight of each sample, train the KNN model, and load the training set data into the model. In this paper, n-dimensional space represents the number of cells involved in the classification, wherein the n-dimensional space for the distance between the two data points $A(x_1, x_2, \cdots x_n)$ and $B(x_1, x_2, \cdots x_n)$ is:

$$d_{A,B} = \sqrt{(y_1 - x_1)^2 + (y_2 - x_2)^2 + \cdots (y_n - x_n)^2} \quad (15)$$

The points A and B are projected in a coordinate system and the cosine values are computed to evaluate the similarity of the two data points, the cosine similarity of the points A and B in n-dimensional space is:

$$Similarity_{A,B} = \frac{\vec{A} \cdot \vec{B}}{\left|\vec{A}\right| \cdot \left|\vec{B}\right|} \tag{16}$$

When two features are similar or identical, the classification requirements are satisfied and the classification result is output.

2.2.3. Model Validation

For each sample in the test set of retired battery packs, the KNN algorithm is used to find the nearest K proximity features, voting is performed according to the categories of proximity features, the samples are assigned to the category with the highest number of votes, and through the cross-validation method, different values of K are taken, and m-weight cross-validation is performed under each value of K. The value with the smallest average error is selected as the optimal solution to output the grouping decision.

With the above method, the battery packs can be categorized using the KNN algorithm according to criteria such as battery health status, shape, volume, price, and brand. The classification performance of the model can be optimized by adjusting the parameters such as the value of K and the distance metric for effective classification of battery packs. The biggest advantage of the KNN algorithm is that it does not need to be re-trained when new samples are added, which makes it ideal for the problem of classifying battery packs after they have been purchased.

2.3. Three-Dimensional Evaluation Modeling of Decommissioned Battery Packs with Objective Functions

In order to accurately predict the dynamic performance of real retired battery packs, a three-dimensional transient electrical energy numerical model was developed. The numerical model was solved by COMSOL version 5.6, a commercial software package based on the finite element method. Firstly, the 3D geometry of the decommissioned battery pack was constructed using Creo and then transferred to COMSOL for numerical simulation as shown in Figure 1. The other components of the decommissioned battery pack group are fully considered in the boundary conditions.

$$Q(t) = \frac{\beta \eta_d}{\alpha_s} \tag{17}$$

where $Q(t)$ is the capacity/m^3 of the decommissioned battery pack, β is the available capacity rate of a single decommissioned battery, α_s is the occupied volume of a single decommissioned battery, and η_d is the utilization efficiency of the whole battery pack.

$$\eta_d = \frac{E_{ch}}{E_{0.5}} \times 100\% \tag{18}$$

where E_{ch} is the total energy discharged from the battery pack from 100% of the state of charge to 20% of the SOC at different cell currents; and $E_{0.5}$ is the total energy discharged from the battery pack from 100% of the state of charge to 20% of the SOC at different cell currents [42].

Measuring the entire volume of the decommissioned battery pack gives the entire capacity of the pack and gives guidance for different pack utilization scenarios.

The objective function is:

$$\min: \quad E = \sum_{m=1}^{n} Battery_m \cdot S'_{P,m} \quad + S_{qw,m}$$
$$s.t. \begin{cases} C_m = C_{r,m} \cdot SOH \\ SOH > 60\% \\ S'_{P,m} = \begin{cases} S_{P,m} \\ S_{P,m} + S_{bbP,m} \quad if \quad S_{b,m} \neq S_{b,m+1} \end{cases} \end{cases} \tag{19}$$

where E indicates the total price of a single battery pack, n is the number of acquired batteries, $C_{r,m}$ is the rated capacity, C_m is the existing capacity of the battery, $S'_{P,m}$ is the acquisition price of the mth lithium battery, and $S_{bbP,m}$ is the price of the mth lithium battery added to the battery pack after treatment. When the existing capacity of the lithium battery is less than 80%, it is retired from the lithium-ion battery and can continue to be utilized in scenarios with low energy density requirements, and when the existing capacity of the lithium battery is less than 60%, the battery no longer has the value of energy storage utilization, and it is not suitable for pack restructuring.

Comparing the economic costs of decommissioned battery packs under the prediction results of the KELM and ELM, as well as the economic costs of decommissioned battery packs in different grouping conditions, it can be seen that the accuracy of the prediction of SOH and the establishment of the grouping conditions are important for the restructuring and utilization of decommissioned battery packs at the same time.

3. Analysis of Results

As all batteries have different charging strategies, and the range of discharge voltage is different, the battery packs need to be classified and processed with the aim of trying to keep the same brand and type of battery in a group. When it is necessary to place batteries from different brands in the same group, the degree of voltage processing needs to be increased to ensure that the output of each battery is balanced, to prolong battery pack life.

Table 3 shows the key parameters of two types of batteries from different brands. In the following analysis, 12 lithium iron phosphate batteries each with a rated capacity of 100 Ah and a cell voltage in the full state of 3.2 V, 2 V when discharged, are connected in parallel to create a battery pack with a rated capacity of 1200 Ah with a standard voltage of 51.2 V. Four different prediction methods are then used to predict the state of the battery charge after discharge of this battery pack. Due to its better thermal stability and long cycle life, the lithium iron phosphate battery is very suitable for reuse after retirement, but due to its lower energy density, it has a greater limitation in the applications. By designing a series of parameters such as the overall physical size, number, and weight of its battery pack, the energy density of the battery pack can be reasonably increased to achieve an efficient and safe strategy for the reuse of retired batteries.

Table 3. Lithium iron phosphate battery parameters.

Lithium Iron Phosphate Battery Parameters	HEQ-JC001 ES-H48100
Cell model	LFP −100 Ah
capacity	100 Ah
voltage	3.2 V
dimension	570 × 525 × 165 mm
Rated voltage	51.2 V
Maximum charging voltage	57.6 V
cut-off voltage	44 V
charging current	0~80 A
Battery weight	45 Kg
appropriate temperature	charge: 2~45 °C discharge: −10~55 °C

Figure 3 shows the process of five discharges of the battery pack. The horizontal coordinate is the process of battery discharge and the vertical coordinate is the battery load state (Ah); the blue line is the battery load state predicted by the ELM, the red line is the battery load state predicted by the KELM, the black line is the actual detected load of the battery, the light blue line is the battery load state predicted by the SSA-KELM, and the purple line is the battery load state predicted by the VMD-SSA-KELM. The consistency between the ELM prediction and the actual load state curve is low, and the consistency is the worst in the case of high load state, which is far lower than the actual value, and its prediction fluctuates up and down in a certain interval, and its prediction stability is poor, and it is more consistent with the actual load curve in the case of low load state. KELM is an extension of ELM, which introduces the kernel technique, and the results are similar to ELM. The kernel technique is more effective in dealing with the nonlinear relationship, which greatly reduces the volatility of the predicted values, and the prediction stability is significantly improved, but the consistency of the model with the actual load curve is still poor in the case of high load state, and it is much lower than the actual curve. VMD-SSA-KELM combines the advantages of VMD, SSA, and KELM, and performs the best in dealing with complex nonlinear battery compliance prediction. Although it still cannot overcome the large periodic error in the discharge cycle, it improves the stability of the prediction and reduces the prediction error. The prediction of the battery state for retired battery packs applies to a lower load state, so the present method is more relevant for the prediction of the maximum load state or the battery life of the retired battery packs' batteries.

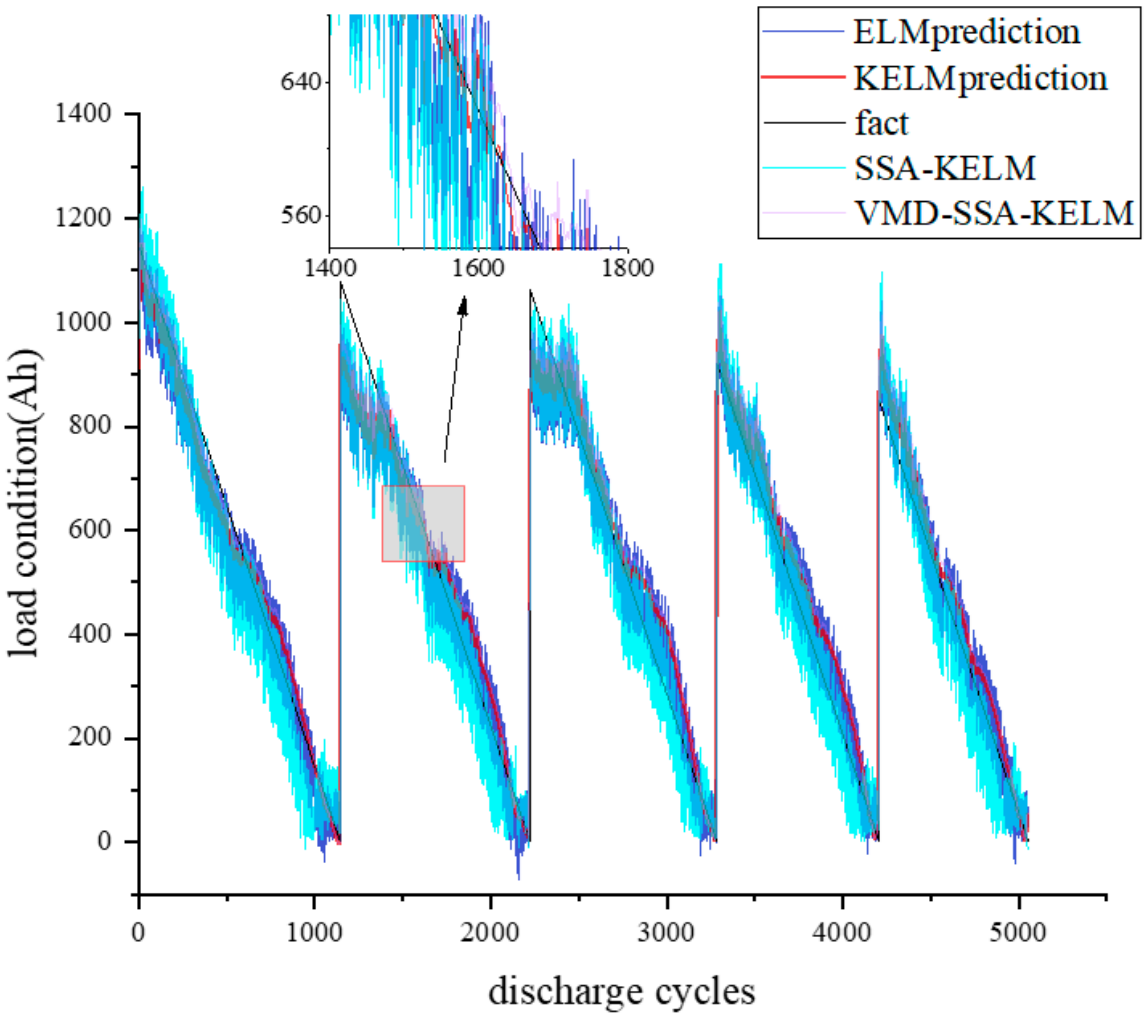

Figure 3. Comparison between the predicted battery load state and the actual load state.

Figure 4 shows the relationship between the actual capacity of the battery and the number of charge/discharge cycles. The capacity of the battery decreases significantly with the increase in the number of charge/discharge cycles of the battery, which shows that the capacity of the battery has an obvious correlation to the prediction of the battery's life, and also further verifies the correctness of selecting the capacity of the battery as the health factor in this paper. Its aging rate can be estimated by calculating the percentage decrease in capacity between the number of consecutive cycles. Locally, there is an obvious abrupt change in battery capacity with an increase in battery charging and discharging cycles, which is due to the short-term rebound of capacity in the resting phase of the battery, which is a normal capacity regeneration phenomenon. The bumps appearing in the graph of the number of cycles can be well avoided by sorting all the capacity values of all the cycles from smallest to largest and finding the ones located in the middle.

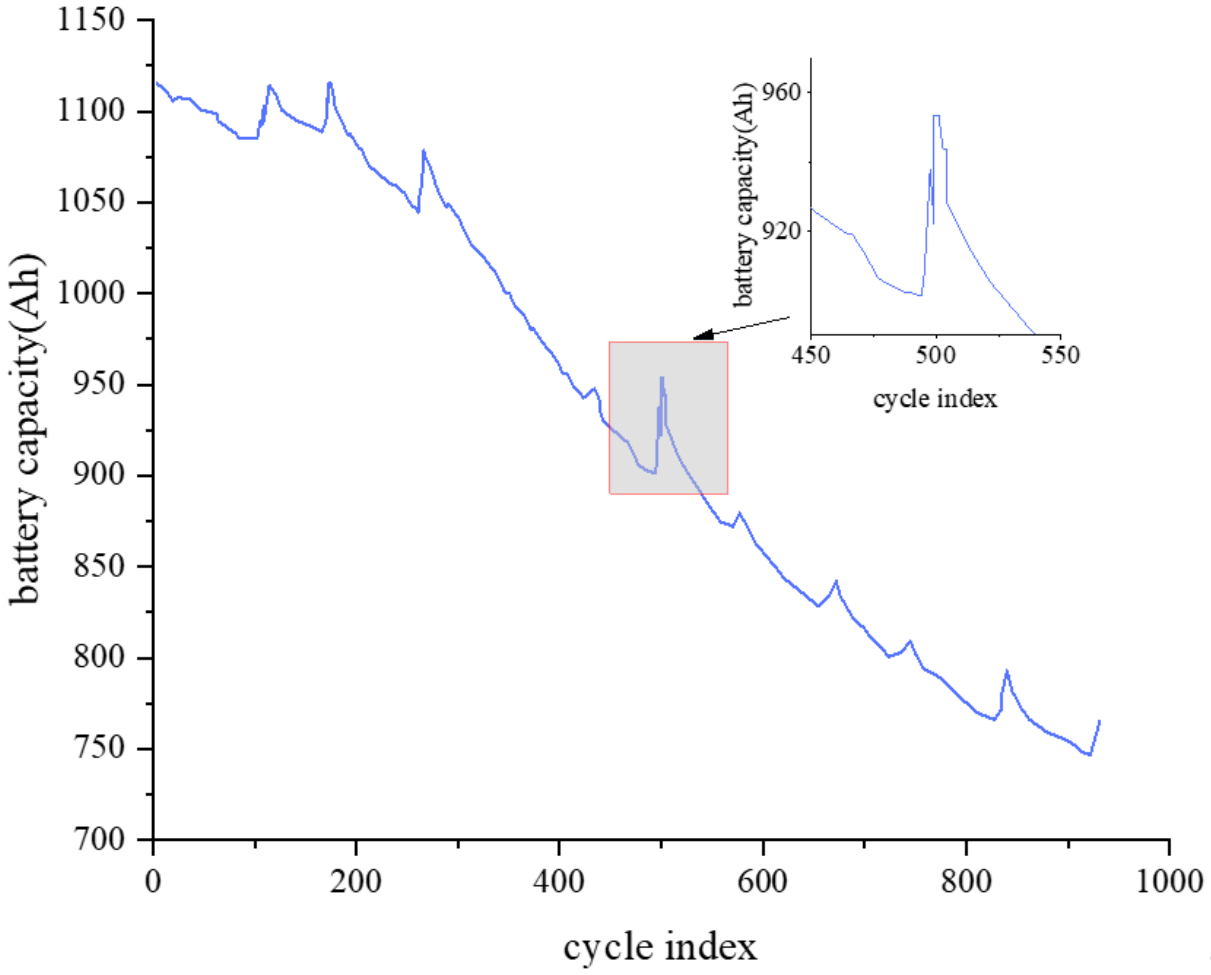

Figure 4. Battery capacity and the number of charge/discharge cycles.

Figure 5 shows a comparison of the error in each predicted battery load. The horizontal coordinate is the sample sampling and the vertical coordinate is the mean square error value.

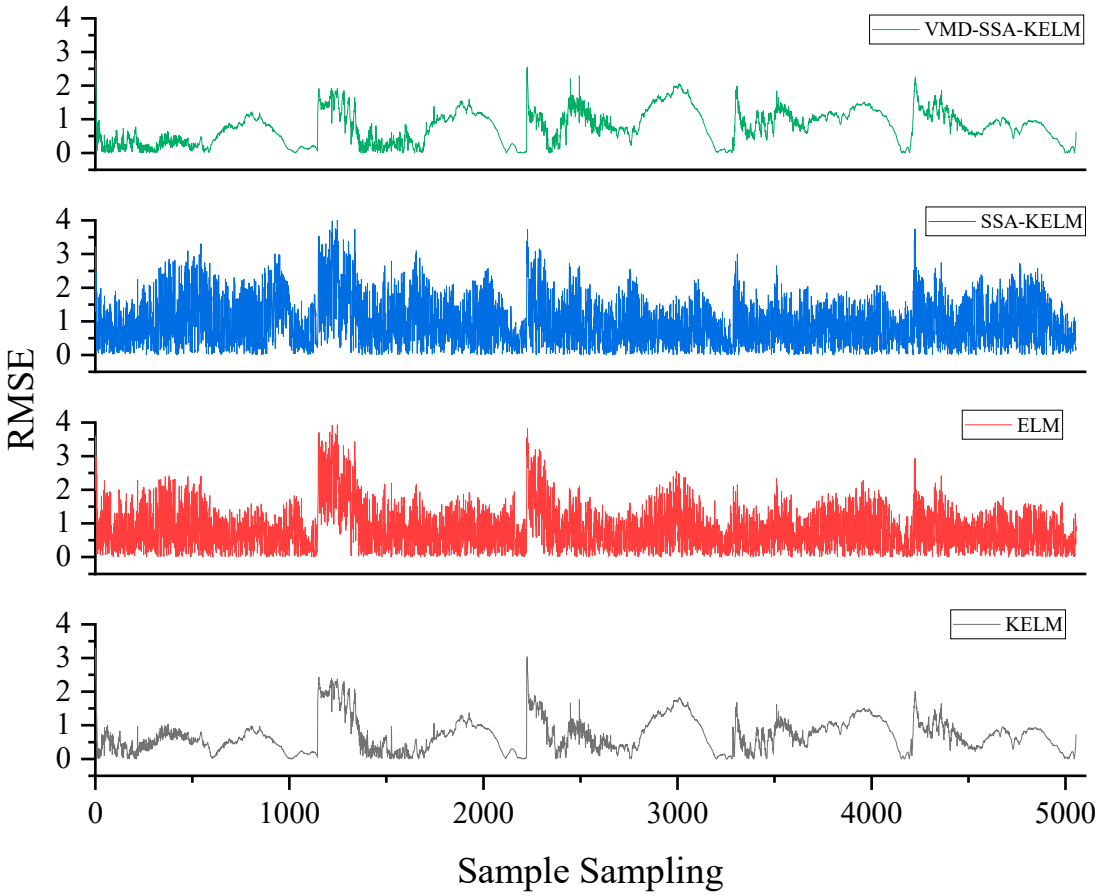

Figure 5. Error in each battery prediction model and actual load state.

SSA-KELM: The RMSE of this method is 2.759 when the sample number is 1, 1.9 when the sample number is 1150, 2.54 when the sample number is 2229, 1.8 when the sample number is 3306, and 2.4 when the sample number is 4425. With an increase in sample number, the error gradually decreases and tends to be constant in a certain interval, which indicates that the method has higher prediction stability and a smaller error with an increase in collected battery discharge samples. In addition, there is a cyclical increase in the error, and the main node of the increase occurs when the samples are in the high load state in the early stage of battery discharging.

SSA-ELM: This method has a RMSE value of 3.2 when the sample number is 1, 3.48 when the sample number is 1150, 3.7 when the sample number is 2229, 2.9 when the sample number is 3306, and 3.68 when the sample number is 4425. The error gradually decreases with an increase in sample number, tends to be constant in a certain interval, and fluctuates up and down a lot in the interval, which indicates that the method has poor prediction stability and large error with an increase in collected battery discharge samples. In addition, there is a cyclical increase in the error, and the main node of the increase occurs when the sample has a high load state in the early stage of battery discharging.

ELM: The RMSE value of this method is 3.59 when the number of samples is 1, 3.6 when the number of samples is 1150, 3.8 when the number of samples is 2229, 2.15 when the number of samples is 3306, and 2.9 when the number of samples is 4425. The error gradually decreases with an increase in sample number and tends to be unchanged in a certain interval; however, the fluctuations within the interval are large, which indicates that the method has poor prediction stability and a larger error with an increase in collected battery discharge samples. The increase in the error is again cyclical, and the main node of the increase occurs when the sample is in the high load state in the early battery discharge. A comparison of the ELM method before and after the optimization of the SSA shows that

the latter has increased the range of the interval of the RMSE, although, in the case of higher negative load states, the error is larger than that in lower negative load states. Although the error is reduced in the case of higher negative load states with this approach, the approach also reduces the stability of the prediction and amplifies the defects of ELM prediction.

KELM: The RMSE of this method is 3.28 at sample number 1, 2.4 at sample number 1150, 2.96 at sample number 2229, 1.6 at sample number 3306, and 1.9 at sample number 4425. The error decreases with an increase in sample number and becomes constant at a certain interval, which indicates that the method has higher prediction stability and a smaller error as more battery discharge samples are collected. There is also a periodic increase in the error, and the main node of the increase occurs when the battery pack is in a higher load state in the early stage of battery discharge. Comparing the KELM prediction errors before and after VMD and SSA optimization, the optimized prediction shows a reduction in the fluctuation interval, improved prediction stability, and a reduction in the cyclical prediction error. It can be seen that the relative prediction error of each method is larger in the case of higher battery loads, and after optimization using the SSA algorithm, the error is further reduced and the prediction stability is high, which makes it more suitable for the prediction of the degradation in decommissioned battery pack performance.

Figure 6 shows a schematic diagram of the battery pack reorganization allocation strategy with X1 as the horizontal axis and X2 as the vertical axis, which represents the distances of each eigenvalue in a two-dimensional planar projection. To calculate this, we determine the number of lithium batteries acquired for classification, determine the group with the lowest number of batteries in the grouped pack, calculate the Euclidean distance between this group and the center of other groups, select the group with the smallest Euclidean distance as the group for removing a single lithium battery, and calculate the Euclidean distances between the features of the center point of the group with the smallest number of lithium batteries and the individual feature points in the group with the smallest Euclidean distance and as the group with the removal of each lithium battery after the clustering of the lithium battery group. The Euclidean distance is sorted, and cells with the smallest distance are moved sequentially from the removed group to the group with the fewest cells, until reaching the rated number in the clustered group.

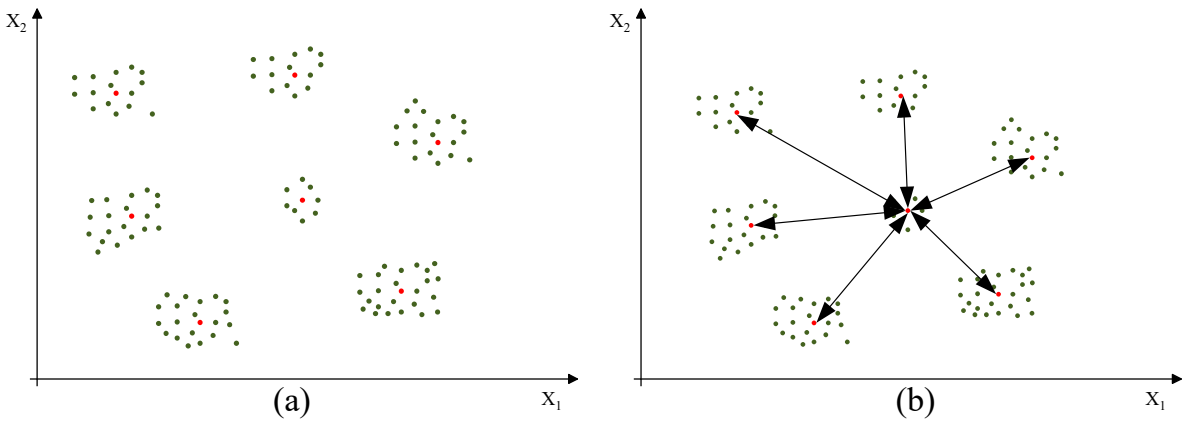

Figure 6. Schematic diagram of the battery pack reorganization allocation strategy. (**a**) battery pack without reorganization allocation strategy (**b**) battery pack with reorganization allocation strategy.

Figure 7 shows the effect of different grouping strategies of battery packs on the difference between the number of cycles and the maximum capacity, where plots (a)–(g) show the relationship between the battery pack attenuation and the number of cycles under the grouping of different strategies, with the horizontal coordinate indicating the number of cycles of the battery pack and the vertical coordinate indicating the capacity of the battery pack that has been attenuated from 90% to 60%. According to the SOH similarly weighted allocation strategy, the number of cycles is around 751 when the battery pack capacity falls

to about 80%, at which point, a plateau phase occurs due to changes in diffusion kinetics within the lithium battery, which is a normal phenomenon. As the battery continues to age, the performance will continue to fall, going through a total of three phases. The first phase is 0–300 cycles, the second phase is 300–700 cycles, and the third stage is more than 700 cycles, which shows that this classification strategy leads to higher battery pack utilization. According to the allocation strategy of SOH similarity, the Sf,b,v,q,c parameters are given more weight, the number of cycles is increased to around 947, and while there is a steep downward trend in the stage from 90% to 80% capacity this is followed by a more gentle fall from 80% to 60% capacity, which indicates that restructuring can prolong the number of times of use of the battery when its health state is lower.

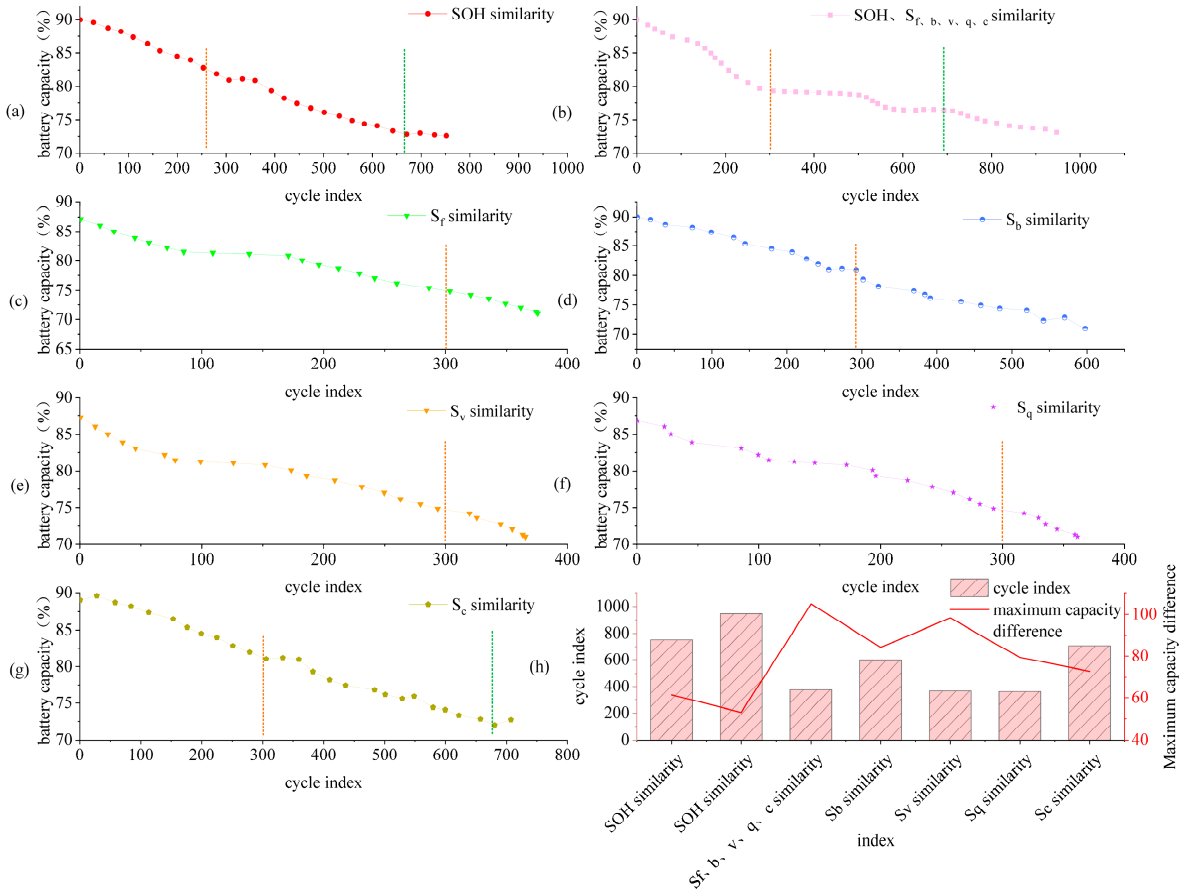

Figure 7. Effect of different grouping strategies. Figure (**a**–**g**) represent the grouping strategies based on the overall weight distribution balance of SOH, Sf,b,v,q,c; where SOH-weight-biased grouping strategy, Sf-weight-biased grouping strategy, Sb-weight-biased grouping strategy, Sv-weight-biased grouping strategy, Sq-weight-biased grouping strategy, and Sc-weight-biased allocation strategy, respectively. Figure (**h**) illustrates the impact of different clustering strategies on the cycle count and maximum capacity difference of the batteries.

Figure 8 presents the three-dimensional evaluation results, where A, B, C, D, E, F, and G represent the grouping strategies based on the overall weight distribution balance of SOH, Sf,b,v,q,c; where SOH-weight-biased grouping strategy, Sf-weight-biased grouping strategy, Sb-weight-biased grouping strategy, Sv-weight-biased grouping strategy, Sq-weight-biased grouping strategy, and Sc-weight-biased allocation strategy, respectively. The pie charts depict the spatial energy density of battery pack groups under different grouping strategies, while the corresponding radar charts below show detailed data such as capacity deviation, number of batteries, cycle times, and spatial energy density.

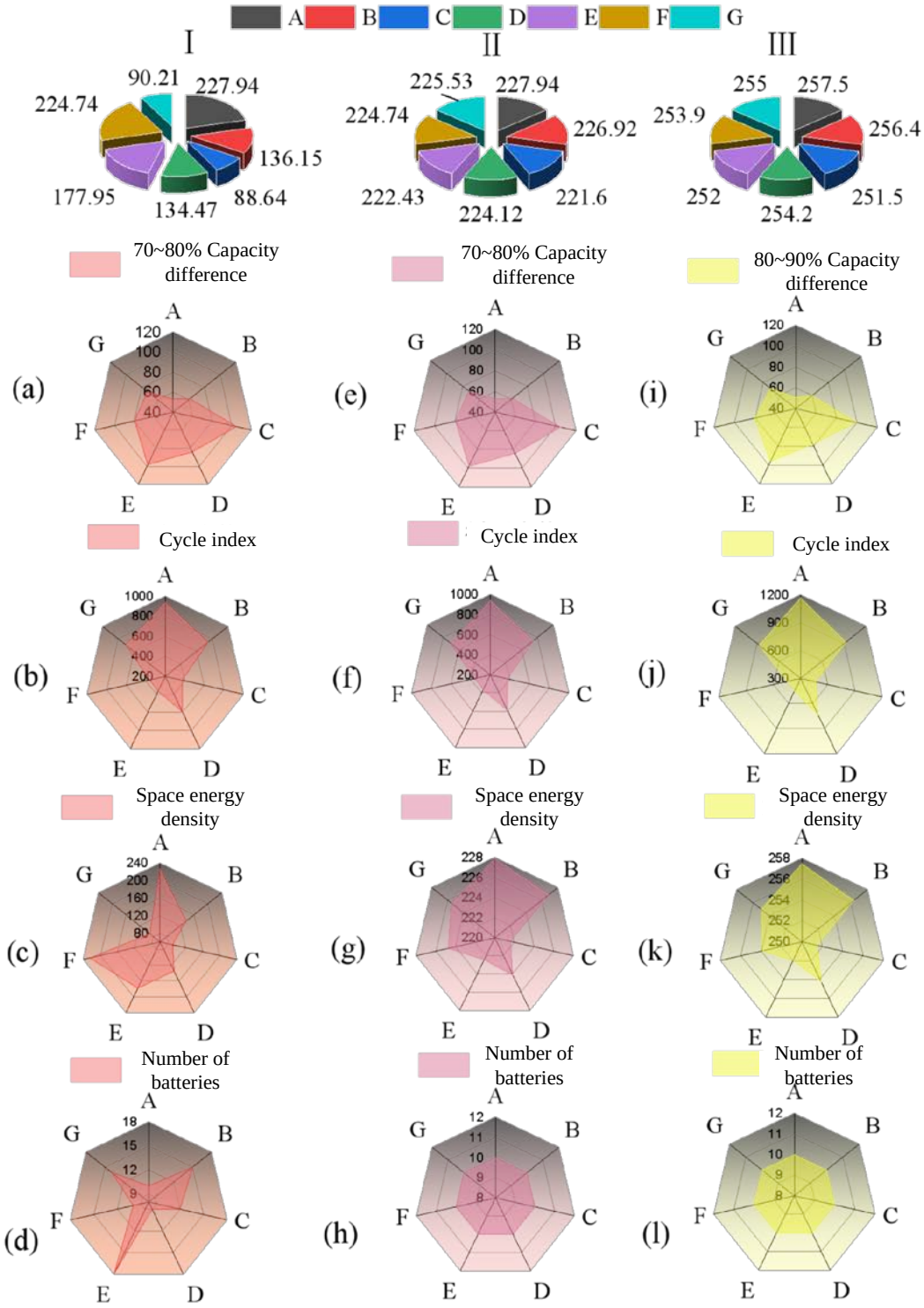

Figure 8. Three-dimensional Evaluation Results. Group (**I**) illustrates the maximum capacity deviation in battery pack groups under different grouping strategies including (**a**–**d**); (**II**) are the number of charge–discharge cycles in battery pack groups under different grouping strategies including (**e**–**h**); (**III**) illustrates the spatial energy density within battery pack groups under different allocation strategies including (**i**–**l**).

In the radar charts, each vertical axis represents the battery pack grouping according to the following strategies:

(a) illustrates the maximum capacity deviation in battery pack groups under different grouping strategies. The similarity values for capacity deviation are as follows:

SOH, Sf,b,v,q,c: 227.9418 Ah, SOH: 136.15474 Ah, Sf: 88.64067 Ah, Sb: 134.47478 Ah, Sv: 177.94607 Ah, Sq: 224.73901 Ah, Sc: 90.21173 Ah. It is evident that the strategy of overall weight distribution balance of SOH, Sf,b,v,q,c is more reasonable as it exhibits the smallest maximum capacity deviation in battery pack groups, making it the most rational grouping strategy. Conversely, the Sc-weight-biased allocation strategy results in a larger capacity deviation in battery pack groups due to deviations in actual capacity during battery degradation, potentially leading to uneven battery output. The SOH-weight-biased grouping strategy shows a smaller capacity deviation, but this is attributed to differences in rated capacity and charge–discharge voltage of batteries from different brands. When using Sf, Sv, and Sq-weight-biased grouping strategies, a larger capacity deviation is observed, indicating that the influence of shape, volume, and mass on capacity deviation is minimal.

(b) depicts the number of charge–discharge cycles in battery pack groups under different grouping strategies. The similarity values for cycle times are as follows: SOH, Sf,b,v,q,c: 947 cycles, SOH: 751 cycles, Sf: 375 cycles, Sb: 597 cycles, Sv: 365 cycles, Sq: 361 cycles, Sc: 707 cycles. It is noticeable that the strategy of overall weight distribution balance of SOH, Sf,b,v,q,c is relatively reasonable, although approximately 33.33% lower than the SOH-similarity strategy, resulting in a larger number of cycle times in battery pack groups, making it a more rational grouping strategy. The Sc-weight-biased allocation strategy leads to a higher number of cycle times in battery pack groups due to potential uneven battery output caused by deviations in actual capacity during battery degradation, thereby reducing the cycle times. The SOH-weight-biased grouping strategy shows a larger number of cycle times, indicating higher similarity in battery capacity and relatively balanced battery output. This method should be considered for achieving lower cycle times. When using Sf, Sv, and Sq-weight-biased grouping strategies, a higher number of cycle times is observed, suggesting that the impact of shape, volume, and mass on cycle times is minimal.

(c) illustrates the spatial energy density within battery pack groups under different allocation strategies, with similarities in SOH, Sf,b,v,q,c at 53.04401 Wh/L, SOH at 61.37571 Wh/L, Sf at 104.97279 Wh/L, Sb at 84.30851 Wh/L, Sv at 98.16719 Wh/L, Sq at 79.2765 Wh/L, and Sc at 72.80347 Wh/L. It can be observed that strategies with balanced overall weight distribution for SOH, Sf,b,v,q,c exhibit a spatial energy density approximately 13.24% lower than the SOH-similar strategy, indicating a reasonable grouping strategy. In strategies where Sc weight is predominant, noticeable differences in maximum capacity within the battery pack groups are observed. Despite similar capacities, deviations in actual capacity occur during battery degradation. Consequently, when these batteries are connected in series to form a larger battery pack, significant disparities in actual capacity may lead to uneven battery output. In strategies where SOH weight is dominant, the capacity differences within the groups are smaller. However, this grouping method does not yield the minimum capacity differences due to variations in rated capacity and charge–discharge voltages among different battery brands. If batteries of the same brand are used, this method should result in smaller capacity discrepancies. Strategies where the Sf, Sv, and Sq weights are prominent result in larger capacity differences within the groups, indicating that shape, volume, and mass have minimal impact on capacity differentials.

In conclusion, based on the three-dimensional evaluation results, we can deduce the impact of different grouping strategies on the performance of battery pack groups and how to allocate batteries reasonably under different strategies to achieve optimal performance.

4. Conclusions and Future Prospects

This study proposes a systematic methodology for the reorganization of retired lithium-ion battery packs. By conducting comprehensive performance assessments on retired battery pack groups, the study seeks more rational battery pack grouping strategies with the aim of increasing the secondary utilization rate of batteries, reducing environmental impact, and providing economically viable solutions for the battery recycling industry. Through precise evaluations of battery health status (SOH), the adoption of KELM, VMD,

an improved sparrow search algorithm (SSA), and a three-dimensional assessment approach, this research significantly enhances the accuracy of battery classification and the performance of reorganized battery packs. The establishment of a three-dimensional assessment model further accurately predicts the dynamic performance of retired battery pack groups, providing crucial insights for the effective reorganization of battery packs.

Results indicate that grouping strategies based on SOH and multi-parameter composite weights can achieve a maximum energy density of 61.37571 Wh/L, increase the cycle count to up to 947 cycles, minimize the maximum capacity difference within groups (227.9418 Ah), and exhibit a high spatial energy density of 53.04401 Wh/L. These outcomes validate the superiority of balanced weight distribution strategies in battery pack reorganization. When KELM is combined with SSA with a sample size of 3306, the root mean square error (RMSE) is reduced to a minimum of 1.6, significantly enhancing prediction stability and accuracy. The three-dimensional assessment results further confirm the significant impact of different grouping strategies on the spatial energy density and utilization efficiency of battery packs. Balanced weight distribution strategies not only perform excellently in capacity difference and cycle count but also provide reasonable performance in spatial energy density, confirming their relevance for applications of battery packs in fields such as electric vehicles and energy storage systems.

While this study has achieved positive results in the reorganization and reuse of retired battery packs, future work will delve into exploring the influence of different battery materials and structures on reorganization outcomes. Additionally, with the rapid development of electric vehicles and energy storage systems, research will extend to broader application scenarios to evaluate and optimize the performance and lifespan of battery packs in real-world operations. This will offer deeper insights for the battery recycling industry and drive ongoing innovation and progress in related technologies.

Author Contributions: Conceptualization, J.S. and H.H.; Methodology, W.C.; Software, L.S.; Validation, L.S.; Formal analysis, N.S.; Investigation, X.G., J.X. and H.H.; Resources, J.J.; Data curation, X.G.; Writing—original draft, W.C.; Writing—review & editing, N.S.; Visualization, J.S.; Project administration, J.X.; Funding acquisition, J.J. All authors have read and agreed to the published version of the manuscript.

Funding: This research received no external funding.

Data Availability Statement: The data that support the findings of this study are available upon request from the corresponding author.

Conflicts of Interest: Author Lei Shen was employed by the Huaian Hongneng Group Corp. The remaining authors declare that the research was conducted in the absence of any commercial or financial relationships that could be construed as a potential conflict of interest.

References

1. Das, K.; Kumar, R.; Krishna, A. Analyzing electric vehicle battery health performance using supervised machine learning. *Renew. Sustain. Energy Rev.* **2024**, *189*, 113967. [CrossRef]
2. Kumar, R.; Das, K. Lithium battery prognostics and health management for electric vehicle application–A perspective review. *Sustain. Energy Technol. Assess.* **2024**, *65*, 103766. [CrossRef]
3. Maheshwari, A.; Navya, R.; Ela, R.; Sabarna, K. Electric Vehicle Battery Health Monitoring System. In Proceedings of the 2024 International Conference on Advances in Data Engineering and Intelligent Computing Systems (ADICS), Chennai, India, 18–19 April 2024; IEEE: Piscataway, NJ, USA, 2024.
4. Pi, X.; Liu, Q. Analysis of the relationship between operating parameters and health state of power batteries. In Proceedings of the Ninth International Conference on Energy Materials and Electrical Engineering (ICEMEE 2023), Guilin, China, 25–27 August 2023; SPIE: San Francisco, CA, USA, 2024.
5. Xia, X.; Yue, J.; Guo, Y.; Lv, C.; Zeng, X.; Xia, Y.; Chen, G. Technologies for Energy Storage Power Stations Safety Operation: Battery State Evaluation Survey and a Critical Analysis. *IEEE Access* **2024**, *12*, 31334–31356. [CrossRef]
6. Zhang, C.; Tian, Y.X.; Han, M.H. Recycling mode selection and carbon emission reduction decisions for a multi-channel closed-loop supply chain of electric vehicle power battery under cap-and-trade policy. *J. Clean. Prod.* **2022**, *375*, 134060. [CrossRef]
7. Melin, H.E.; Rajaeifar, M.A.; Ku, A.Y.; Kendall, A.; Harper, G.; Heidrich, O. Global implications of the EU battery regulation. *Science* **2021**, *373*, 384–387. [CrossRef]

8. Turner, J.M.; Nugent, L. Charging up battery recycling policies: Extended producer responsibility for single-use batteries in the European union, Canada, and the United States. *J. Ind. Ecol.* **2016**, *20*, 1148–1158. [CrossRef]
9. Tang, Y.; Zhang, Q.; Li, Y.; Wang, G.; Li, Y. Recycling mechanisms and policy suggestions for spent electric vehicles' power battery-A case of Beijing. *J. Clean. Prod.* **2018**, *186*, 388–406. [CrossRef]
10. Chen, X. Research on China's power battery recycling and reuse policy. *IEEE Access* **2024**, *7*, 94–96.
11. Hao, Y. Implications of the EU Battery Policy Upgrade on the Construction of Circular Economy in China. *IEEE Access* **2024**, *4*, 19–24.
12. Liu, J.M.S.; Smith, K.; Wang, C.Y. Real-time reconfiguration-based all-cell flexibility and capacity maximum utilization of second-life batteries. *J. Power Sources IEEE Trans. Transp. Electrif.* **2023**, *450*, 227794.
13. Chiu, Y.C.M.; Hsu, C. Reuse of Retired Lithium-Ion Batteries (LIBs) for Electric Vehicles (EVs) from the Perspective of Extended Producer Responsibility (EPR) in Taiwan. *Resour. Conserv. Recycl. World Electr. Veh. J.* **2023**, *171*, 105659.
14. Wang, P.L.J.; Zhang, S.; Sun, J. A machine learning-based state of health prognosis model for lithium-ion batteries. *Appl. Energy IEEE Access* **2023**, *260*, 114395.
15. Yu, H.; Dai, H.; Tian, G.; Xie, Y.; Wu, B.; Zhu, Y.; Li, H.; Wu, H. Big-data-based power battery recycling for new energy vehicles: Information sharing platform and intelligent transportation optimization. *IEEE Access* **2020**, *8*, 99605–99623. [CrossRef]
16. Zhang, B.; Li, J.; Yue, X. Driving mechanism of power battery recycling systems in companies. *Int. J. Environ. Res. Public Health* **2020**, *17*, 8204. [CrossRef] [PubMed]
17. Yu, W.; Guo, Y.; Shang, Z.; Zhang, Y.; Xu, S. A review on comprehensive recycling of spent power lithium-ion battery in China. *Etransportation* **2022**, *11*, 100155. [CrossRef]
18. He, W.; King, M.; Luo, X.; Dooner, M.; Li, D.; Wang, J. Technologies and economics of electric energy storages in power systems: Review and perspective. *Adv. Appl. Energy* **2021**, *4*, 100060. [CrossRef]
19. Song, K.; Hu, D.; Tong, Y.; Yue, X. Remaining life prediction of lithium-ion batteries based on health management: A review. *J. Energy Storage* **2023**, *57*, 106193. [CrossRef]
20. Zhang, M.; Xu, C.; Huang, Z. Essential Safety Mechanism and Case Analysis of Energy Storage System Based on Dynamic Reconfigurable Battery Network. *Energy Storage Sci. Technol.* **2022**, *11*, 2442.
21. Zou, F. *Research on Lithium-Ion Battery Health State Assessment and Remaining Useful Life Prediction Technology*; Nanjing University of Aeronautics and Astronautics: Nanjing, China, 2016.
22. Cheng, P. Joint Estimation Method of State of Health (SOH) and Remaining Useful Life (RUL) of Lithium-Ion Battery Based on Health Feature Parameters. *Energy Storage Sci. Technol.* **2022**, *42*, 1523–1534.
23. Wu, Z.; Jiang, Q.; Zhu, M.; Chen, C.; Wang, D.; Shi, X. Current Research Status of Lithium-Ion Battery Health State Prediction. *Energies* **2020**, *8*, 486–492.
24. Zhang, Z. A Review of Big Data-Driven Methods for Estimating the Health Status of Power Batteries. *IEEE Access* **2023**, *59*, 151–168.
25. Jalili, M.; Chitsaz, A.; Hashemian, M.; Rosen, M.A. Economic and environmental assessment using emergy of a geothermal power plant. *Energy Convers. Manag.* **2021**, *228*, 113666. [CrossRef]
26. Cao, X. Quantum Particle Swarm Optimization-based Nuclear Extreme Learning Machine for Remote Sensing Image Classification. *IEEE Access* **2023**, *41*, 642–648.
27. Wang, G.; Sun, L.; Wang, A.; Jiao, J.; Xie, J. Lithium battery remaining useful life prediction using VMD fusion with attention mechanism and TCN. *J. Energy Storage* **2024**, *93*, 112330. [CrossRef]
28. Meng, Q.; Huang, Y.; Li, L.; Wu, F.; Chen, R. Smart batteries for powering the future. *Joule* **2024**, *8*, 373. [CrossRef]
29. Luo, Z. Method and Characteristics Study of Power Battery Charging and Discharging Efficiency Testing. *IEEE Access* **2019**, *16*, 7–9+24.
30. Li, G.; Lu, M.; Lai, S.; Li, Y. Research on Power Battery Recycling in the Green Closed-Loop Supply Chain: An Evolutionary Game-Theoretic Analysis. *Sustainability* **2023**, *15*, 10425. [CrossRef]
31. Faraji-Niri, M.; Rashid, M.; Sansom, J.; Sheikh, M. Accelerated state of health estimation of second life lithium-ion batteries via electrochemical impedance spectroscopy tests and machine learning techniques. *J. Energy Storage* **2023**, *58*, 106295. [CrossRef]
32. Bustos, R.; Gadsden, S.A.; Biglarbegian, M.; Alshabi, M. Battery State of Health Estimation Using the Sliding Interacting Multiple Model Strategy. *Energies* **2024**, *17*, 536. [CrossRef]
33. Jiao, Z.; Ma, J.; Zhao, X.; Zhang, K.; Li, S. A methodology for state of health estimation of battery using short-time working condition aging data. *J. Energy Storage* **2024**, *82*, 110480. [CrossRef]
34. Renold, A.P.; Kathayat, N.S. Comprehensive Review of Machine Learning, Deep Learning, and Digital Twin Data-Driven Approaches in Battery Health Prediction of Electric Vehicles. *IEEE Access* **2024**, *12*, 43984–43999. [CrossRef]
35. Safavi, V.; Bazmohammadi, N.; Vasquez, J.C.; Guerrero, J.M. Battery State-of-Health Estimation: A Step towards Battery Digital Twins. *Electronics* **2024**, *13*, 587. [CrossRef]
36. Bai, X.; Peng, D.; Chen, Y.; Ma, C.; Qu, W.; Liu, S.; Luo, L. Three-dimensional electrochemical-magnetic-thermal coupling model for lithium-ion batteries and its application in battery health monitoring and fault diagnosis. *Sci. Rep.* **2024**, *14*, 10802. [CrossRef] [PubMed]
37. Hou, S. International Experience and Inspirations on Recycling and Reuse of Waste Power Lithium Batteries. *Energy Storage Mater.* **2023**, *51*, 83–86.

38. Kou, F.; Yang, T.; Luo, X.; Men, H. Lithium Battery State of Charge Estimation Based on ISSA-ELM Algorithm. *J. Power Supply* **2024**, *2*, 1–8.
39. Sun, Z.; Luo, D.; Wang, R.; Li, Y.; Yan, Y.; Cheng, Z.; Chen, J. Evaluation of energy recovery potential of solar thermoelectric generators using a three-dimensional transient numerical model. *Energy* **2022**, *256*, 124667. [CrossRef]
40. Song, S.-J.; Wang, Z.-H.; Lin, X.-F. Research on SOC estimation of LiFePO4 batteries based on ELM. *Chin. J. Power Sources* **2018**, *42*, 806–808.
41. Xue, J. Research and application of a novel swarm intelligence optimization technique: Sparrow search algorithm. *Syst. Sci. Control Eng.* **2020**, *8*, 1–10.
42. Sbordone, D.A.; Di Pietra, B.; Bocci, E. Energy Analysis of a Real Grid Connected Lithium Battery Energy Storage System. *Energy Procedia* **2015**, *75*, 1881–1887. [CrossRef]